



Morphological basis of glossy red plumage colours

JEAN-PIERRE ISKANDAR¹, CHAD M. ELIASON^{1,2}, TIM ASTROP^{1,3}, BRANISLAV IGIC¹, RAFAEL MAIA^{1,4} and MATTHEW D. SHAWKEY^{1*}

¹Integrated Bioscience Department, The University of Akron, 175 E. Mill St., Akron, OH 44325-3908, USA

²Departments of Geological Sciences and Integrative Bioscience, University of Texas at Austin, 2305 Speedway Stop C1160, Austin, TX 78712, USA

³Department of Biology & Biochemistry, University of Bath, Bath, BA2 7AY, UK

⁴Department of Ecology, Evolution and Environmental Biology, Columbia University, 1200 Amsterdam Avenue, New York, NY 10027, USA

Received 18 February 2016; revised 16 March 2016; accepted for publication 16 March 2016

Brightly coloured feathers, including the brilliant reds produced by carotenoids, are sometimes shiny in appearance. Gloss is a common property of materials and usually arises through specular reflection from smooth, flat surfaces. However, the production of gloss on red feathers has never been examined. In the present study, we compared the optical and structural properties of glossy and matte carotenoid-based red feathers of multiple species to identify the proximate basis for their glossiness. Although specular reflectance did not differ between glossy and matte feathers, diffuse reflectance was lower in glossy than in matte feathers, leading to a higher contrast gloss. Compared to matte feathers, glossy red feathers had thicker barbs with a flatter and more homogeneous morphology, consistent with expectations, as well as thicker outer keratin cortices. Moreover, glossiness was predicted by a principal component regression using these same morphological traits. We demonstrate that the gloss of carotenoid-based red feathers is produced at least in part by a smooth, flattened barb microstructure and an enhanced nanostructure, illustrating a novel colour-producing interaction that neither pigment, nor microstructure could alone attain. How the ecology and evolution of species with glossy red feather differ from those with typical matte red feathers represent rich areas for future study. © 2016 The Linnean Society of London, *Biological Journal of the Linnean Society*, 2016, **00**, 000–000.

KEYWORDS: feathers – iridescence – pigments – sexual selection – structural colour.

INTRODUCTION

Bright avian plumage colours are some of the most conspicuous signals found in animals, playing important roles in intra- and interspecific communication, as well as camouflage (Hill & McGraw, 2006). Understanding the mechanisms underlying the production and maintenance of feather colours is critical to understanding their function (Prum, 2006; Shawkey, Morehouse & Vukusic, 2009a; Shawkey, Pillai & Hill, 2009b; Wilts *et al.*, 2014), the constraints on their production (McGraw, 2006; Galván & Alonso-Alvarez, 2008; Shawkey *et al.*, 2015), and their evolution across

species (Stoddard & Prum, 2011; Maia, Rubenstein & Shawkey, 2013a; Maia *et al.*, 2013b; Eliason, Maia & Shawkey, 2015). Traditionally, feather colours have been classified as either pigment-based (produced by selective absorption of certain wavelengths of light by molecules, mainly melanins and carotenoids) or structural (produced by differential scattering and interference as light interacts with material of varying refractive indices; Prum, 2006). However, the structural and pigmentary components of coloration often interact to produce colours. For example, in budgerigar (*Melopsittacus undulatus*, Gould, 1840) feathers, a pigment selectively absorbs blue wavelengths, enhancing the green colour produced by the nanostructured spongy matrix of keratin and air (D'Alba, Kieffer & Shawkey, 2012). Indeed, variation in colours traditionally interpreted as 'pigment-based' can often be structurally derived (Shawkey & Hill, 2005; Jacot

*Corresponding author. Current address: Department of Biology, Terrestrial Ecology Group, University of Ghent, Ledeganckstraat 35, Ghent 9000 Belgium. E-mail: matthew.shawkey@ugent.be

et al., 2010; Evans & Sheldon, 2012; San-Jose *et al.*, 2013) and this variation might be as relevant in signalling and interactions as that controlled by pigment deposition itself.

Most studies of coloration have focused on examining brightness, hue and saturation, and have overlooked other properties. Gloss, the quality of mirror-like or specular reflectance characteristics of material, is usually produced by smooth polished surfaces (Hunter, 1937) and is a common component of avian feathers (Toomey *et al.*, 2010). A few recent studies have focused on gloss in natural materials by attempting to quantify it (Toomey *et al.*, 2010), as

well as identify the morphological features underlying its production (Maia, D'Alba & Shawkey, 2011; Vignolini *et al.*, 2012; Igit *et al.*, 2015). Gloss is noticeable on darkly coloured surfaces, such as melanin-based black feathers, where specular highlights contrast markedly with the dark diffusely reflected colour. However, gloss can also be observed on feathers coloured by carotenoids.

From the velvety bib of the house finch (*Haemorrhous mexicanus*, Müller, 1776) to the fiery crests of woodpeckers (Piciformes), carotenoid-based red feathers can vary dramatically in their glossiness (Fig. 1). However, the mechanisms producing gloss

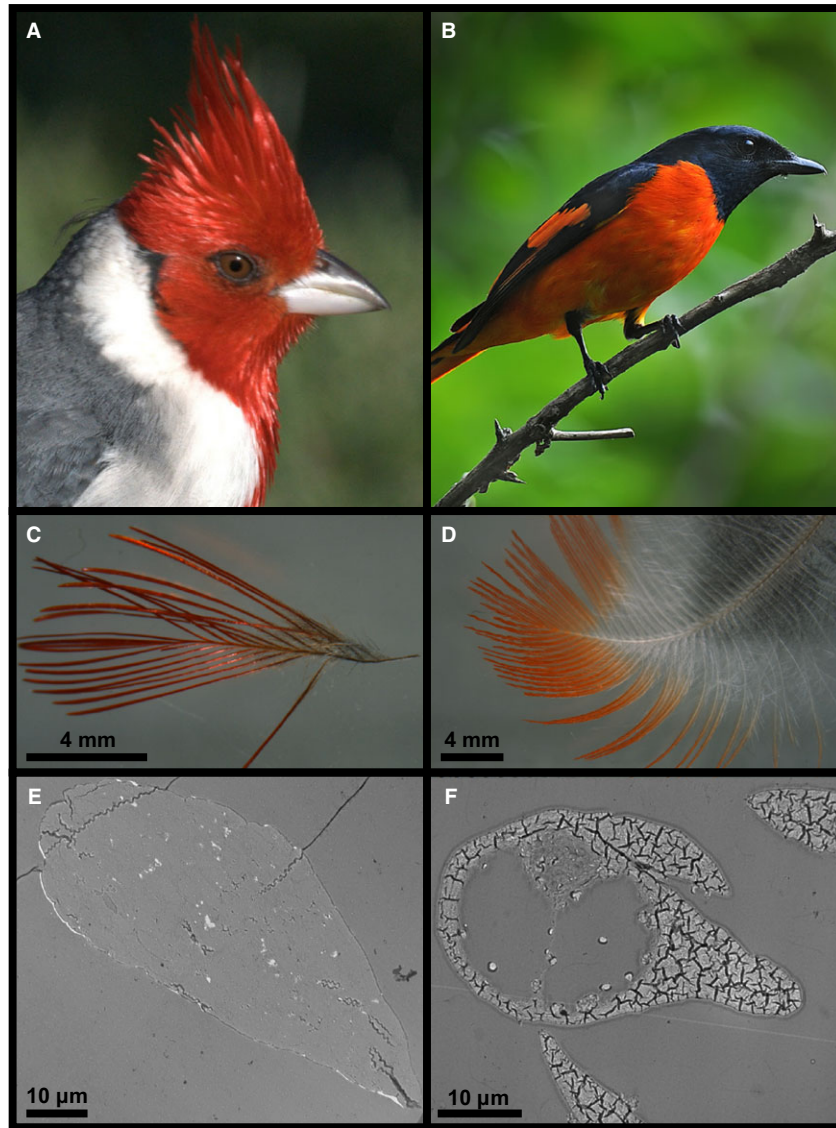


Figure 1. Comparison of representative glossy and matte red feathers. A, B, photographs of red-crested cardinal (*Paroaria coronata*) and scarlet minivet (*Pericrocotus speciosus*). C, D, single feathers from the crown of red-crested cardinal and breast of scarlet minivet. E, F, transmission electron microscopy image of cross section of barbs, as well as barbules in (F), from feathers of the crown of red-crested cardinal and breast of scarlet minivet.

on red feathers may differ from those producing gloss on black feathers. This is because the latter are affected by the degree of organization and continuity in the barbule layer formed by the rod-shaped melanin-containing organelles (melanosomes) and by the thickness of the keratin layer overlaying it (Maia *et al.*, 2011). Carotenoids and other red pigments, however, are not found in organelles and, instead, are diffusely mixed within the keratin matrix of the feather (Shawkey & Hill, 2005; Shawkey *et al.*, 2009a,b). Thus, gloss is probably produced by different mechanisms in carotenoid-pigmented feathers.

The present study aimed to characterize gloss in red-pigmented feathers and to identify the underlying mechanisms responsible for its production and variation. We quantified gloss using angle-resolved spectrophotometry and compared it between carotenoid-based red feathers that were visually classified as either glossy or matte. We then identified the morphological basis of gloss by relating it to the macro- and nanoscale morphology of these feathers.

MATERIAL AND METHODS

SAMPLE COLLECTION

Samples of red bird feathers were collected from the ornithological collection of The University of Akron and the Cleveland Museum of Natural History. Twenty-six samples from several avian families were collected and visually classified by four different observers as either matte ($N = 13$) or glossy ($N = 13$) during sampling. Seven feathers of each bird were collected per species (Table 1; see also Supporting information, Table S1): five were used for spectrophotometry measurements, and the remainder were embedded for light microscopy and transmission electron microscopy (see below).

COLOUR MEASUREMENTS

We stacked and taped five feathers directly on top of one another to a holder with a matte black velvet background and measured their reflectance between 300 and 700 nm (i.e. the bird-visible spectrum) using an Avantes AvaSpec-2048 spectrometer, an AvaLight-XE pulsed xenon light source and an Avantes WS-2 white standard as a reference. We measured feathers in stacks rather than on study skins to minimize variation (e.g. as a result of curvature of the bird's body). Feathers were not cleaned before measurement. Gloss can be affected by both specular and diffuse reflectance, and so we measured both on the same samples using standard techniques. To quantify specular reflectance, we took reflectance measurements using two separate probes both placed at 60° from the plane normal using a block

holder (AFH-15; Avantes), averaging 10 scans at one pulse per 100 ms integration time. Measuring at high angles minimizes scattering from the bulk material (i.e. pigments, keratin fibres; Hunter, 1937) and thus maximizes captured gloss. We measured reflectance with the light source oriented parallel to the barbs. A subsample measured with the light source orthogonal to the barbs showed a higher reflectance for both glossy and matte feathers (see Supporting information, Figure S1), indicating that sample orientation would similarly affect both sets of samples and therefore probably not affect our conclusions.

We measured diffuse reflectance using an integrating sphere (AvaSphere-50-REFL; Avantes) equipped with a black gloss trap to exclude specular reflectance (AvaSphere-GT50; Avantes). We took three measurements (a mean of 10 scans at five pulses per 500 ms integration time) for each species, moving the probe holder slightly between measurements, and averaged the spectra to account for variation in reflectance along the feather surface. We applied loess smoothing (smoothness parameter of 0.25) to reduce spectral noise and calculated the total brightness of each spectrum as the mean relative reflectance over 300–700 nm. We then calculated contrast gloss as the ratio of mean specular to mean diffuse reflectance (Hunter's contrast gloss; Hunter, 1937). All spectral analyses were performed in R (R Core Team, 2013) using the pavo package (Maia *et al.*, 2013a).

FEATHER MICROSTRUCTURE ANALYSIS

We examined feather morphology using light microscopy (LM) and transmission electron microscopy (TEM) to identify the morphology associated with gloss production by red feathers. We embedded the feathers using a standard protocol described previously (Shawkey *et al.*, 2003), trimmed blocks with an S6 EM-Trim 2 (Leica Microsystems), and cut 80-nm thick ultrathin sections with an Ultra 45 diamond knife (Diatome Ltd) on an UC-6 ultramicrotome (Leica Microsystems). We prepared 100-nm thick samples for TEM analysis and 500-nm thick sections for LM. To clearly observe interior structure and pigment distribution, we stained cross-sections with either toluene for LM or uranyl acetate and lead citrate for TEM. We viewed the cross-sections using a Leica light microscope and a JEM-1230 transmission electron microscope (JEOL) at an operating voltage of 120 kV.

We used IMAGEJ (<http://fiji.sc/Fiji>) to measure variation in feather morphology. We measured barb thickness (area in μm^2 occupied by a cross-section); barb curvature at the exposed (visible) portion of the barb surface where we observed maximal gloss (arc

Table 1. Feathers used in our comparisons of the colour and morphology of glossy and matte red feathers

Species	Type	Patch	Family
Scarlet minivet (<i>Pericrocotus flammeus</i>)*	Matte	Breast	Campephagidae
Red-crested cardinal (<i>Paroaria coronata</i>)	Glossy	Head	Cardinalidae
Northern cardinal (<i>Cardinalis cardinalis</i>)	Matte	Breast	Cardinalidae
Rose-breasted grosbeak (<i>Pheucticus ludovicianus</i>)	Matte	Breast	Cardinalidae
Guianan red cotinga (<i>Phoenicircus carnifex</i>)*	Glossy	Head	Cotingidae
Guianan red cotinga (<i>Phoenicircus carnifex</i>)	Matte	Breast	Cotingidae
Common redpoll (<i>Carduelis flammea</i>)	Glossy	Crown	Fringillidae
Cassin's finch (<i>Haemorhous cassinii</i>)*	Glossy	Crown	Fringillidae
House finch (<i>Carpodacus mexicanus</i>)	Matte	Rump	Fringillidae
Red-winged blackbird (<i>Agelaius phoeniceus</i>)	Matte	Wing	Icteridae
Red-breasted blackbird (<i>Sturnella militaris</i>)*	Matte	Epaulet	Icteridae
Double-toothed barbet (<i>Lybius bidentatus</i>)	Glossy	Throat	Lybiidae
Crimson sunbird (<i>Aethopyga siparaja</i>)	Matte	Back	Nectariniidae
Painted redstart (<i>Myioborus pictus</i>)	Matte	Breast	Parulidae
Amherst pheasant (<i>Chrysolophus amherstiae</i>)	Glossy	Belly	Phasianidae
Yellow-bellied sapsucker (<i>Sphyrapicus varius</i>)	Glossy	Crown	Picidae
Red-headed woodpecker (<i>Melanerpes erythrocephalus</i>)	Glossy	Crown	Picidae
Wire-tailed manakin (<i>Pipra filicauda</i>)*	Glossy	Crown	Pipridae
Red-whiskered bulbul (<i>Pycnonotus jocosus</i>)	Glossy	Cheek	Pycnonotidae
Chestnut-eared araçari (<i>Pteroglossus castanotis</i>)	Matte	Breast	Ramphastidae
Crimson-backed tanager (<i>Ramphocelus dimidiatus</i>)	Glossy	Rump	Thraupidae
Red-rumped paradise tanager (<i>Tangara chilensis</i>)	Glossy	Rump	Thraupidae
Scarlet tanager (<i>Piranga olivacea</i>)	Matte	Breast	Thraupidae
Scarlet ibis (<i>Eudocimus ruber</i>)	Matte	Breast	Threskiornithidae
Resplendent quetzal (<i>Pharomachrus mocinno</i>)	Matte	Breast	Trogonidae
Vermilion flycatcher (<i>Pyrocephalus rubinus</i>)	Glossy	Crown	Tyrannidae

*Representative species used in the Supporting information (Fig. S1).

length divided by the radius of a circle fit to a set of points along the edge of a barb profile; Berresford & Rockett, 2013); the aspect ratio of barbs (length divided by width, measured at the outermost points of a barb profile); barb density (measured as the number of barbs divided by the rachis length); and the length of the barb ramus covered by barbules (as a proportion of total ramus length). We did not focus on barbule morphology because they were sparse or absent on our glossy feathers (as on structurally-coloured blue feathers; Shawkey *et al.*, 2005) and, in most cases when present, showed no evidence of three-dimensional (3D) structuring (e.g. a ribbon shape) that may affect gloss production. In all cases, we only measured variables from red-coloured barbs. In addition to feather surface structure, the amount of light reflected from a material may also depend on the thickness of the outermost keratin layer of feather barbules or barbs, which could act as a thin-film reflector (Prum, 2006). Therefore, in addition to quantifying barb microstructure, we also measured the mean thickness of the keratin cortex at the outer edge of barbs from TEM images.

GEOMETRIC MORPHOMETRICS OF BARB CROSS-SECTIONAL SHAPE

Because of the subcircular outline of the sectioned barbs and a lack of multiple clear anatomically homologous features, traditional landmark-based morphometric techniques (Bookstein, 1982) would be inappropriate for these samples. The analysis of outlines via eigenshape shape analysis (*sensu* Macleod, 1999) has been successfully implemented in many recent studies (Ubukata *et al.*, 2009; Astrop, 2011; Astrop *et al.*, 2012; Wilson *et al.*, 2013a,b) to assess morphological variation within and between taxa where such homologous features are absent.

Eigenshape analyses operate via the conversion of the digitized outline of an individual specimen into equidistant, Cartesian (x, y) coordinates. These digitized coordinates are then transformed (removing size, scale, and rotation from the analysis) into a shape function as angular deviations (phi function: ϕ ; Zahn & Roskies, 1972) that describe the shape of the curve.

Outlines of the samples were digitized into 20 equidistant points from the apex of curvature at the

dorsum of the barb (type II landmark) using TPSDIG2 (Rohlf, 2001). Eigenshape analyses were performed using FORTRAN routines written by Norman MacLeod (Natural History Museum, London). The eigenshape functions in the freely available PAST software (Harper & Ryan, 2001) were implemented for shape visualization.

STATISTICAL ANALYSIS

We used linear models to test whether feather morphology affects both observer classifications and spectrophotometric measurements of glossiness. First, we tested whether human classified glossy and matte feather differed with respect to measurements of contrast gloss, diffusely reflected brightness, and specularly reflected brightness. Second, we tested whether human classified glossy and matte feather differed with respect to barb thickness, barb curvature, barb cortex thickness, barb density, barbule coverage, and aspect ratio of barbs.

To avoid potential problems associated with multicollinearity among morphological measurements, we used principal component (PC) analysis on the correlations matrix of morphological measurements to reduce them to several orthogonal axes that explain the greatest amount of total variance (see Supporting information, Table S2). Prior to PC analysis, we natural log-transformed barb thickness and curvature, and arcsine-transformed barbule coverage. We also log-transformed contrast gloss, diffuse reflectance, and specular reflectance prior to our analyses.

We included the first four PC axes, which collectively explained 90% of the total morphological variance, in our analyses. For example, the first PC axis compared barb thickness, cortex thickness, and density with barb curvature, barb aspect ratio, and barbule coverage, whereas the second PC compared barb thickness, curvature, and cortex thickness with barb aspect ratio (see Supporting information, Table S2). We used penalized maximum likelihood logistic regression to test whether morphological variation explained by the first four PC axes influences the probability that human vision classifies a feather as glossy versus matte (see Supporting information, Table S3). Next, we used linear models to test whether morphological variation explained by the first four PC axes influences contrast gloss, as well as diffuse and specular reflectance (see Supporting Information, Table S3). We used the same analyses to compare contrast gloss to eigenshapes.

Because shared common ancestry between species can influence the outcomes of comparative analyses, we repeated PCA and inferential analyses at the same time as controlling for phylogenetic relatedness

among species. In these analyses, the amount of phylogenetic non-independence between samples was accounted for by simultaneously computing a measure of phylogenetic signal in the residuals of the models (λ in the case of linear models and α for logistic regressions: Revell, 2010; Ives & Garland, 2010). However, as expected from an evolutionarily highly labile trait (low phylogenetic signal) and our sampling design, including phylogenetic information in our analyses did not affect our conclusions (see Supporting information, Tables S4, S5). Therefore, we report the results from nonphylogenetically controlled models below.

Finally, we used permutational multivariate analysis of variance (MANOVA) based on distance metrics to test for differences across eigenshape axes between human classified matte and glossy feathers, and assessed homogeneity of variance among glossy and matte feathers by comparing distances from points to group centroids. All statistical analyses were conducted in R, version 3.2.2 (R Core Team, 2013.). We fit linear models using the `lm()` function in the base package of R and the penalized maximum likelihood logistic regression model using the `logistf` package (Ploner *et al.*, 2013). We conducted phylogenetic PC analysis using the `phytools` package (Revell, 2012) and phylogenetically controlled general linear models using the `phylolm` package (Ho & Ane, 2014). We conducted permutational MANOVAs using the `vegan` package (Oksanen *et al.*, 2015).

RESULTS

REFLECTANCE AND GLOSS

Our visual classification of feathers as ‘matte’ or ‘glossy’ reflected quantifiable differences in their reflectance properties (Fig. 2A). Diffuse brightness of human-classified matte feathers was more than twice as high as that for glossy feathers [mean \pm SE log (brightness) for glossy versus matte: -0.78 ± 0.13 , $t_{23} = -6.06$, $P < 0.001$] (Fig. 2B), although the two groups did not differ in their specular reflectance [mean \pm SE log(brightness) for glossy versus matte: 0.10 ± 0.17 , $t_{23} = 0.60$, $P = 0.56$] (Fig. 2C). As a consequence, their contrast gloss significantly differed by a magnitude similar to that of diffuse reflectance measurements [mean \pm SE log(contrast gloss) for glossy versus matte: 0.88 ± 0.14 , $t_{23} = 6.23$, $P < 0.001$] (Fig. 2D).

GLOSS AND FEATHER MORPHOLOGY

The morphology of human-classified matte and glossy red feathers differed. Barbs of glossy feathers were flatter, thicker, less covered by barbules, and

Table 2. Mean \pm SE for measurements on the morphology of human classified glossy ($N = 13$) and matte red feathers ($N = 12$)

	Glossy	Matte
Barb thickness (μm^2)	3272.67 \pm 665.86	1473.49 \pm 440.51
Barb curvature (radians)	29.14 \pm 4.38	105.11 \pm 13.61
Mean barb cortex thickness (nm)	91.08 \pm 8.68	68.66 \pm 4.93
Barbule coverage (proportion)	0.31 \pm 0.07	0.89 \pm 0.07
Barb aspect ratio (length/breadth)	2.31 \pm 0.32	2.28 \pm 0.19

had thicker cortices (PC1: mean \pm SE glossy versus matte log-odds ratio: 1.75 \pm 0.78, $\chi_1^2 = 16.65$, $P < 0.0001$) (Table 2; see also Supporting information, Table S3).

Feather morphology also affected the reflectance properties of red feathers. Diffuse reflectance decreased [mean \pm SE log(brightness) versus PC1: -0.23 ± 0.04 , $t_{20} = -5.28$, $P < 0.0001$] (Fig. 3A; see

also Supporting information, Table S3), whereas contrast gloss increased [mean \pm SE log(contrast gloss) versus PC1: 0.26 ± 0.05 , $t_{20} = 5.04$, $P < 0.0001$] (Fig. 3D; see also Supporting information, Table S3) as barbs were flatter, thicker, with thicker cortices, and less covered by barbules. In addition, diffuse reflectance decreased as barbs were rounder with lower aspect ratios [mean \pm SE log(contrast gloss) versus PC2: -0.13 ± 0.06 , $t_{20} = -2.41$, $P = 0.03$] (Fig. 3B; see also Supporting information, Table S3). By contrast, specular reflectance was not significantly associated with any morphological traits (all $P > 0.05$) (Fig. 3C; see also Supporting information, Table S3).

GLOSS AND BARB GEOMETRIC MORPHOMETRICS

Matte and glossy barbs differed significantly in their overall shape based on the first three axes of shape variation (permutational MANOVA: $F_{1, 23} = 4.26$, $P = 0.005$, $r^2 = 15.65\%$) (Fig. 4) and did not differ in levels of within-group variation (analysis of multivariate homogeneity of group dispersions: $F_{1, 23} = 1.79$, $P = 0.19$). The first three eigenshapes accounted for 64% of the observed variation within the dataset. Eigenshape 1 highlighted changes in

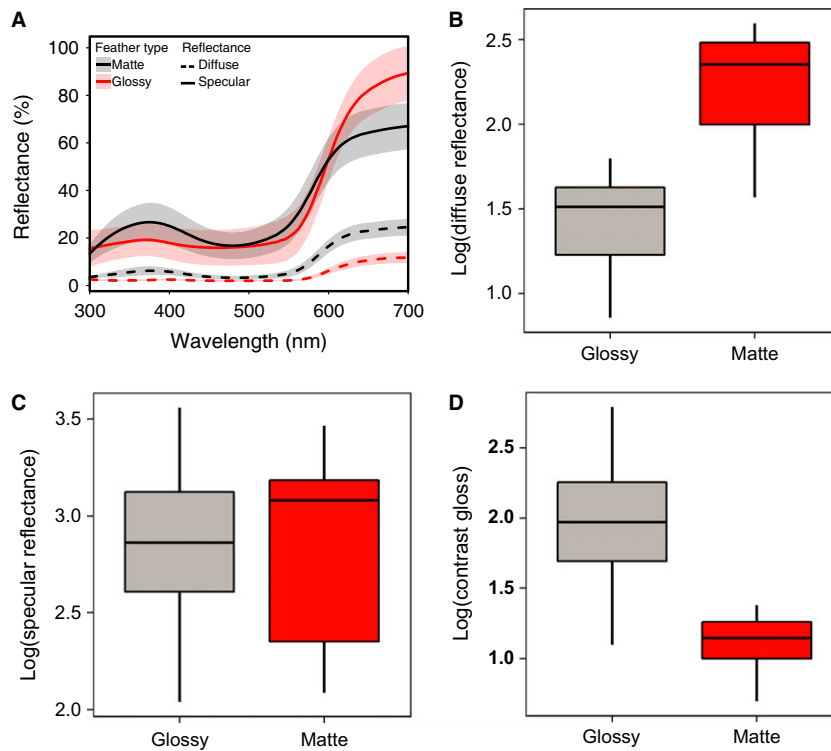


Figure 2. Quantitative assessment of glossiness in red feathers. A, mean specular (solid lines) and diffuse reflectance spectra (dashed lines) of glossy (red) and matte feathers (black); shaded bands indicate the SE. B–D, Boxplots of log diffuse reflectance (B), log specular reflectance (C), and log contrast gloss (specular/diffuse reflectance) (D) in glossy and matte feathers.

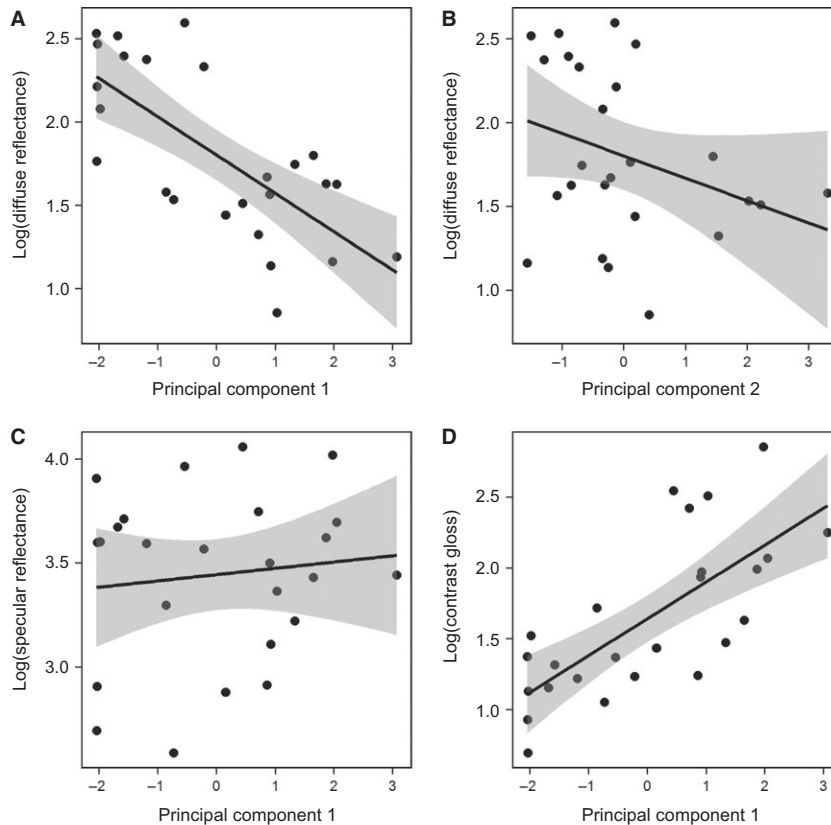


Figure 3. Relationship between morphology and spectral properties of red feathers. Conditional plots showing the relationship between log diffuse brightness and principal component (PC)1 (A) or PC2 (B), log specular brightness and PC1 (C), and log contrast gloss and PC1 (D). PC 1 compared the barb thickness, cortex thickness, and density with barb curvature, barb aspect ratio, and barbule coverage and accounted for 39% of total morphological variance, whereas PC 2 compared the barb thickness, curvature, and cortex thickness with barb aspect ratio and accounted for 24% of total morphological variance (see Supporting information, Table S1). Shaded regions are 95% confidence bands.

shape of the ventral width of the barb and accounted for 30% of the shape variation. Eigenshape 2 described changes in the width toward the dorsal apex of the barb and accounted for 22% of the shape variation. Eigenshape 3 described changes in the overall width, centred toward the middle of the barb, and accounted for 12% of the captured variation in shape. The third eigenshape (describing differences on the curvature of the midsection of the barb cross-section) (Fig. 4) was the only significant predictor of contrast gloss such that glossy feathers had flatter (less concave) barb midsections (mean \pm SE estimate: 0.23 ± 0.11 , $t_{20} = 2.11$, $P < 0.05$) (Fig. 4; see also Supporting information, Table S6).

DISCUSSION

Gloss has been studied in human hair (Keis, Ramaprasad & Kamath, 2004), synthetic material (Wicks, 2011), eggs (Igic *et al.*, 2015; Maurer and Cassey

2011), plants (Vignolini *et al.*, 2012), and feathers (Toomey *et al.*, 2010; Maia *et al.*, 2011). Glossy surfaces in all these cases are typified by high specular brightness. Thus, we expected glossy red feathers to have a higher specular brightness than matte feathers. Instead, they had a lower diffuse reflectance, leading to a higher contrast gloss as defined by the ratio of specular to diffuse reflectance. Our morphological analyses of glossy and matte feathers revealed distinct differences in barb shape that were strongly associated with matte and glossy feather types. Our analyses showed that large, flat barbs reflect light more strongly in the specular direction, whereas smaller, curved barbs reflect light diffusely in multiple directions. One possible reason for the positive relationship between barb size and glossiness is that large barbs produced a greater surface area for light reflection (Marschner *et al.*, 2003; Keis *et al.*, 2004), whereas a lower barb density would cause diffuse scattering from barb edges. The negative relationship between barb ramus curvature and

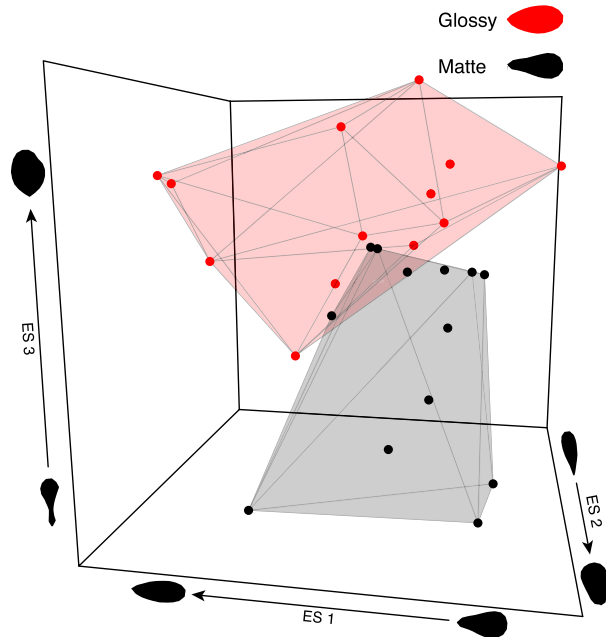


Figure 4. Three dimensional morphospace of barb shape constructed using the first three major axes of variation captured via eigenshape analysis. Polygonal convex hulls illustrate occupied space of both glossy and matte groupings. Silhouettes on axes represent barb shapes at extremes of either eigenshape.

glossiness is consistent with optical theory because curved (convex) surfaces scatter light more diffusely than flat surfaces, leading to lower gloss (Barkas, 1939; Hecht & Zajac, 1974). A similar effect has recently been reported in dragonfly wings (Nixon, Orr & Vukusic, 2015). The presence of barbules may increase diffuse scattering, which could potentially explain why reduction in barbule coverage reduced diffuse brightness and contrast gloss.

The positive relationship between gloss and cortex thickness indicates that nanostructure also plays a role in gloss production. Interestingly, the buttercup flower (*Ranunculus repens*, Linnaeus, 1758) produces a glossy yellow colour through specular reflection from a smooth outer surface containing pigments (Vignolini *et al.*, 2012). However, carotenoids in red feathers are distributed throughout their barb, and so it is unlikely that they share this mechanism with buttercups. Keratin cortices in glossy red feathers are approximately 65 nm thinner on average than those that contribute to glossy colour in black feathers (Maia *et al.*, 2011) but could nevertheless produce bird-visible colour through thin-film interference (Hecht & Zajac, 1974). However, the refractive index contrast between the cortex and the underlying keratin matrix in red feathers is probably low, unlike that between the cortex and

melanosomes in glossy black feathers. Thus, reflectance from this layer should be weak, although more data on refractive indices (Wilts *et al.*, 2014) are needed to test this idea.

Although not measured in the present study, variation in carotenoid concentration may also affect glossiness. Higher concentrations of carotenoids should strongly reduce diffuse reflectance because carotenoids absorb light (McGraw, 2006). This would lead to a darker background reflectance that would provide contrast and thereby increase the visibility of specular reflectance. We hypothesized that this may explain why diffuse brightness of glossy feathers was lower than, and specular brightness was unexpectedly similar to, that of matte feathers. However, chroma of wavelengths known to be absorbed by carotenoids (i.e. R450-550/R300-700; McGraw, 2006) was not correlated with any of these variables (see Supporting information, Tables S3, S5). Analyzing the relative carotenoid content of these feathers will enable us to test this hypothesis more directly in future studies.

Taken together, these results imply that barb morphology, barbule presence/absence, and carotenoid concentration collectively contribute to the production of gloss. However, the precise optics of this system and how these feather characteristics affect gloss production in relation to feather position and placement on birds remain to be examined. 3D structuring of barbules may also influence the reflectance properties of red feathers, and could be examined in future studies using 3D tomography techniques. However, the barbules of the glossy red feathers in the present study often lacked barbules, or had a limited distribution near the rachis, suggesting that barbule morphology contributes minimally to their gloss production. Furthermore, the unexpectedly high levels of variation in barb ramus shape (exemplified in Fig. 1) observed in the present study raise further questions about the diversity, development, and genetic determinants of these relatively unexplored feather barb morphologies. For example, it will be interesting to investigate whether other glossy carotenoid-containing (e.g. yellow tail feathers of cedar waxwings *Bombycilla cedrorum*) and/or structurally-coloured feathers (e.g. blue feathers of fairy bluebirds *Irena spp.*) feature similar modifications.

Animal signals are complex, multimodal phenotypes characterized by their colour, form, and motion (Grether, Kolluru & Nersissian, 2004). Carotenoid-based colours in birds are diverse (Stoddard & Prum, 2011) and are considered to have evolved through sexual selection for their signalling functions (Hill, 2006). In addition to the considerable variation in the form and colour of carotenoid-based plumage traits (Stoddard & Prum, 2011), the results of the present study suggest that the dynamic character of

glossiness is similarly variable and broadly distributed throughout birds with carotenoid-based colour (Table 1). Our mechanistic work shows that the glossiness of red feathers is produced by numerous aspects of feather morphology, and can therefore vary independently of chromatic colour attributes (e.g. hue), potentially allowing birds to convey unique information to receivers about their quality or motivation to mate. Testing whether and how these different colour attributes (hue and glossiness) act as redundant signals or interact to determine mating success remains to be explored (Hebets & Papaj, 2005). Furthermore, several studies have shown that carotenoid-based colours can be altered by preening and soiling (Surmacki & Nowakowski, 2007; Lopez-Rull, Pagan & Garcia, 2010), as well as bacterial degradation (Shawkey *et al.*, 2009b). Whether these factors independently affect gloss represents an interesting direction for future research.

Glossiness is a highly directional trait (changing with viewing angle) and birds may be able to flash these signals on and off similar to iridescent traits (Osorio & Ham, 2002; Meadows *et al.*, 2011). Interestingly, many glossy feathers are found on crests (Table 1), which can sometimes be dynamically raised and lowered during signalling. Recent work suggests that directional signals cause a strong link between the environment (e.g. lighting conditions) and signalling behaviour (Dakin & Montgomerie, 2009; Siscu *et al.*, 2013) that might drive the evolution of display behaviour. Glossiness may therefore play an important but largely overlooked role in the sexual selection of carotenoid-based bird colours (Toomey *et al.*, 2010; Maia *et al.*, 2011). These results increase our understanding of the structural mechanisms behind glossiness and provide a framework for future studies on the ecology and evolution of glossy, carotenoid-coloured feathers in birds.

ACKNOWLEDGEMENTS

We thank Dr Andrew Jones and the Cleveland Museum of Natural History for access to specimens, the Shawkey laboratory group; and Dr Richard Prum and two anonymous reviewers for their helpful comments. This work was funded by HFSP RGY-0083 and AFOSR FA9550-13-1-0222 (to MDS).

REFERENCES

Astrop TI. 2011. Phylogeny and evolution of mecochiridae (Decapoda: Reptantia: Glypheoidea): an integrated morphometric and cladistic approach. *Journal of Crustacean Biology* **31**: 114–125.

- Astrop T, Park L, Brown B, Weeks SC. 2012.** Sexual discrimination at work: spinicaudatan ‘clam shrimp’ (Crustacea: Branchiopoda) as a model organism for the study of sexual system evolution. *Palaeontologia Electronica* **15**: 2.20A.
- Barkas WW. 1939.** Analysis of light scattered from a surface of low gloss into its specular and diffuse components. *Proceedings of the Physical Society* **51**: 274.
- Berresford GC, Rockett AM, eds. 2013.** *Applied calculus*, 6th edn. Boston, MA: Brooks/Cole.
- Bookstein F. 1982.** Foundations of morphometrics. *Annual Review of Ecology and Systematics* **13**: 451–470.
- Dakin R, Montgomerie R. 2009.** Peacocks orient their courtship displays towards the sun. *Behavioral Ecology and Sociobiology* **63**: 825–834.
- D’Alba L, Kieffer L, Shawkey MD. 2012.** Relative contributions of pigments and biophotonic nanostructures to natural color production: a case study in budgerigar (*Melopsittacus undulatus*) feathers. *The Journal of Experimental Biology* **215**: 1272–1277.
- Eliason CM, Maia R, Shawkey MD. 2015.** Modular color evolution in birds facilitated by a complex nanostructure. *Evolution* **69**: 357–367.
- Evans SR, Sheldon BC. 2012.** Quantitative genetics of a carotenoid-based color: heritability and persistent natal effects in the Great Tit. *American Naturalist* **179**: 79–94.
- Galván I, Alonso-Alvarez C. 2008.** An intracellular antioxidant determines the expression of a melanin-based signal in a bird. *Public Library of Science One* **3**: e3335.
- Grether GF, Kolluru GR, Nersissian K. 2004.** Individual colour patches as multicomponent signals. *Biological Reviews* **79**: 583–610.
- Harper D, Ryan P. 2001.** PAST: paleontological statistics software package for education and data analysis. *Palaeontologia Electronica* **4**: 1–9.
- Hebets EA, Papaj DR. 2005.** Complex signal function: developing a framework of testable hypotheses. *Behavioral Ecology and Sociobiology* **57**: 197–214.
- Hecht E, Zajac A. 1974.** *Optics*. New York, NY: Addison-Wesley.
- Hill GE. 2006.** Female mate choice for ornamental coloration. In: McGraw KJ, Hill GE, eds. *Bird coloration*, Vol. II. Cambridge, MA: Harvard University Press, 137–200.
- Hill GE, McGraw KJ, eds. 2006.** *Bird Coloration, Vol. 1: mechanisms and Measurement*. Cambridge, MA: Harvard University Press.
- Ho LST, Ane C. 2014.** A linear-time algorithm for Gaussian and non-Gaussian trait evolution models. *Systematic Biology* **63**: 397–408.
- Hunter RS. 1937.** Methods of determining gloss. *Journal of Research of the National Bureau of Standards* **18**: 19–39.
- Igic B, Fechey-Lippens DC, Chan A, Hanley D, Brennan P, Grim T, Waterhouse GIN, Hauber ME, Shawkey MD. 2015.** A nanostructural basis for gloss of avian eggshells. *Journal of The Royal Society Interface* **12**: 1210–1215.
- Ives AR, Garland T. 2010.** Phylogenetic logistic regression for binary dependent variables. *Systematic Biology* **59**: 9–26.

- Jacot A, Romero-Diaz C, Tschirren B, Richner H, Fitze PS. 2010.** Dissecting Carotenoid from Structural Components of Carotenoid-Based Coloration: a Field Experiment with Great Tits (*Parus major*). *American Naturalist* **176**: 55–62.
- Keis K, Ramaprasad K, Kamath Y. 2004.** Studies of light scattering from ethnic hair fibers. *Journal of Cosmetic Science* **55**: 49–63.
- Lopez-Rull I, Pagan I, Garcia C. 2010.** Cosmetic enhancement of signal coloration: experimental evidence in the house finch. *Behavioral Ecology* **21**: 781–787.
- Macleod N. 1999.** Generalizing and extending the eigen-shape method of shape space visualization and analysis. *Paleobiology* **25**: 107–138.
- Maia R, D'Alba L, Shawkey MD. 2011.** What makes a feather shine? A nanostructural basis for glossy black colours in feathers. *Proceedings of the Royal Society of London Series B, Biological Sciences* **278**: 1973–1980.
- Maia R, Rubenstein DR, Shawkey MD. 2013a.** Key ornamental innovations facilitate diversification in an avian radiation. *Proceedings of the National Academy of Sciences of the United States of America* **110**: 10687–10692.
- Maia R, Eliason CM, Bitton PP, Doucet SM, Shawkey MD. 2013b.** Pavo: an R package for the analysis, visualization and organization of spectral data. *Methods in Ecology and Evolution* **4**: 906–913.
- Marschner SR, Jensen HW, Cammarano M, Worley S, Hanrahan P. 2003.** Light scattering from human hair fibers. *ACM Transactions on Graphics (TOG)* **22**: 780–791.
- Maurer G, Cassey P. 2011.** Evaluation of a glossmeter for studying the surface appearance of avian eggs. *Journal of Ornithology* **152**: 209–212.
- McGraw KJ. 2006.** Mechanics of melanin-based coloration. In McGraw KJ, Hill GE, eds. *Bird coloration, Vol. II*. Cambridge, MA: Harvard University Press, 243–294.
- Meadows MG, Morehouse NI, Rutowski RL, Douglas JM, McGraw KJ. 2011.** Quantifying iridescent coloration in animals: a method for improving repeatability. *Behavioral Ecology and Sociobiology* **65**: 1317–1327.
- Nixon MR, Orr AG, Vukusic P. 2015.** Wrinkles enhance the diffuse reflection from the dragonfly *Rhyothemis resplendens*. *Journal of the Royal Society Interface* **12**: 749–755.
- Oksanen J, Guillaume Blanchet F, Kindt R, Legendre P, Minchin PR, O'Hara RB, Simpson GL, Solymos P, Henry M, Stevens H, Wagner H. 2015.** vegan: Community Ecology Package. R package, Version 2.3-1. <http://CRAN.R-project.org/package=vegan>
- Osorio D, Ham A. 2002.** Spectral reflectance and directional properties of structural coloration in bird plumage. *Journal of Experimental Biology* **205**: 2017–2027.
- Ploner M, Dunkler D, Southworth H, Heinze G. 2013.** logistf: Firth's bias reduced logistic regression. R package, Version 1.21. Available at: <http://CRAN.R-project.org/package=logistf>
- Prum RO. 2006.** Anatomy, physics and evolution of avian structural colors. In McGraw KJ, Hill GE, eds. *Bird coloration, Vol. I*. Cambridge, MA: Harvard University Press, 295–353.
- R Core Team. 2013.** R: a language and environment for statistical computing, Version 3.0.1. Vienna, Austria: R Foundation for Statistical Computing.
- Revell LJ. 2010.** Phylogenetic signal and linear regression on species data. *Methods in Ecology and Evolution* **1**: 319–329.
- Revell LJ. 2012.** Phytools: an R package for phylogenetic comparative biology (and other things). *Methods in Ecology and Evolution* **3**: 217–223.
- Rohlf JF. 2001.** TPSDig2: A Program for Landmark Development and Analysis New York: Department of Ecology and Evolution, State University of New York, Stony Brook. (<http://life.bio.sunysb.edu/morph/>).
- San-Jose LM, Granado-Lorencio F, Sinervo B, Fitze PS. 2013.** Iridophores and not carotenoids account for chromatic variation of carotenoid-based coloration in common lizards. *American Naturalist* **181**: 396–409.
- Shawkey MD, Hill GE. 2005.** Carotenoids need structural colours to shine. *Biology Letters* **1**: 121–124.
- Shawkey MD, Estes AM, Siefferman LM, Hill GE. 2003.** Nanostructure predicts intraspecific variation in ultraviolet-blue plumage colour. *Proceedings of the Royal Society of London Series B, Biological Sciences* **270**: 1455–1460.
- Shawkey MD, Estes AM, Siefferman LM, Hill GE. 2005.** The anatomical basis of sexual dichromatism in non-iridescent ultraviolet-blue structural coloration of feathers. *Biological Journal of the Linnean Society* **85**: 259–271.
- Shawkey MD, Morehouse NI, Vukusic P. 2009a.** A protean palette: colour materials and mixing in birds and butterflies. *Journal of the Royal Society Interface* **6**: S221–S231.
- Shawkey MD, Pillai SR, Hill GE. 2009b.** Do feather-degrading bacteria affect sexually-selected plumage color? *Naturwissenschaften* **96**: 123–128.
- Shawkey MD, D'Alba L, Xiao M, Schutte M, Buchholz R. 2015.** Ontogeny of an iridescent nanostructure composed of hollow melanosomes. *Journal of Morphology* **276**: 378–384.
- Siscu P, Manica LT, Maia R, Macedo RH. 2013.** Here comes the sun: multimodal displays are associated with sunlight incidence. *Behavioral Ecology and Sociobiology* **67**: 1633–1642.
- Stoddard MC, Prum RO. 2011.** How colorful are birds? Evolution of the avian plumage color gamut. *Behavioral Ecology* **22**: 1042–1052.
- Surmacki A, Nowakowski JK. 2007.** Soil and preen waxes influence the expression of carotenoid-based plumage coloration. *Naturwissenschaften* **22**: 829–835.
- Toomey MB, Butler MW, Meadows MG, Taylor LA, Fokidis HB, McGraw KJ. 2010.** A novel method for quantifying the glossiness of animals. *Behavioral Ecology and Sociobiology* **64**: 1047–1055.
- Ubukata T, Tanabe K, Shigeta Y, Maeda H, MAPES RH. 2009.** Eigenshape analysis of ammonoid sutures. *Lethaia* **43**: 266–277.
- Vignolini S, Thomas MM, Kolle M, Wenzel T, Rowland A, Rudall PJ, Baumberg JJ, Glover BJ, Steiner U. 2012.** Directional scattering from the glossy flower of *Ranunculus*: how the buttercup lights up your chin. *Journal of The Royal Society Interface* **9**: 1295–1301.

- Wicks ZW. 2011.** Coatings. In: Seidel A, ed. *Processing and finishing of polymeric materials, Vol. 1*. Hoboken, NJ: Wiley Inc., 387–460.
- Wilson L, Furrer H, Stockar R, Sanchez-Villagra M. 2013a.** A quantitative evaluation of evolutionary patterns in opercle bone shape in Saurichthys (Actinopterygii: Saurichthyidae). *Palaeontology* **56**: 901–915.
- Wilson L, Colombo M, Reinhold H, Salzburger W, Sanchez-Villagra M. 2013b.** Ecomorphological disparity in an adaptive radiation: opercular bone shape and stable isotopes in Antarctic icefishes. *Ecology and Evolution* **3**: 3166–3182.
- Wilts BD, Michielsen K, De Raedt H, Stavenga DG. 2014.** Sparkling feather reflections of a bird-of-paradise explained by finite-difference time-domain modeling. *Proceedings of the National Academy of Sciences of the United States of America* **111**: 4363–4368.
- Zahn C, Roskies R. 1972.** Fourier descriptions for plane closed curves. *IEEE Transactions on Computers*. **C21**: 269–281.

SUPPORTING INFORMATION

Additional Supporting Information may be found online in the supporting information tab for this article:

Figure S1. Mean specular reflectance spectra for five representative species (indicated in Table 1) measured at three different viewing geometries and orientations relative to the spectrometer set-up.

Table S1. Specimen numbers and collection dates of feathers used in the present study.

Table S2. Summary of loadings and the total variance explained by individual axes from a nonphylogenetic principal component analysis on the morphological measurements on the glossy and matte red feathers.

Table S3. Summary tables for nonphylogenetically controlled models comparing the morphology of red feathers in relation to their probability of being glossy, as well as the levels of contrast gloss, diffuse, and specular brightness.

Table S4. Summary of loadings and the total variance explained by individual axes from a phylogenetic principal component analysis on the morphological measurements on the glossy and matte red feathers.

Table S5. Summary tables for phylogenetically controlled models comparing the morphology of red feathers with respect to levels of contrast gloss, as well as diffuse and specular brightness.

Table S6. Summary table for linear model comparing the contrast gloss of red feathers with respect to the geometric morphology of barb from eigenshape analysis.